106
9-2-80

ANL-80-15

Dw: 1692

ANL-80-15

MASTER

OFFICIAL USE ONLY

DEVELOPMENT OF A 25-CM ANNULAR CENTRIFUGAL CONTACTOR

by

R. A. Leonard, G. J. Bernstein, and A. A. Ziegler

~~EXPORT CONTROLLED INFORMATION~~

~~Contains technical data whose export is restricted by statute. Violations may result in administrative, civil, or criminal penalties. Limit dissemination to U.S. Department of Energy, DOE contractors, and DOE Cleared personnel, and to other U.S. Government agencies. The cognizant program manager must approve other dissemination. This notice shall not be separated from the attached document.~~

~~Mary Hale 8-17-2006~~

~~Reviewer (signature) Date~~

Distribution of this report is Unlimited David Hamrin OSTI 8/1/2019

~~APPLIED TECHNOLOGY~~

~~APPLIED TECHNOLOGY~~

~~Any Further Distribution by any Holder of this Document or of Other Data Therein to Third Parties Representing Foreign Interests, Foreign Governments, Foreign Companies and Foreign Subsidiaries or Foreign Divisions of U. S. Companies Should Be Coordinated with the Director, Nuclear Power Development Division, Department of Energy. (U83-86)~~

Over 25 years old.
(B. Layton) 6/2006

ARGONNE NATIONAL LABORATORY

ARGONNE NATIONAL LABORATORY, ARGONNE, ILLINOIS

Prepared for the U. S. DEPARTMENT OF ENERGY under Contract W-31-109-Eng-38

~~RELEASED FOR ANNOUNCEMENT IN ALDR. Distribution limited to participants in the Consolidated Fuel Reprocessing Program. Others request from Program Mgr. CFRP, OROO.~~

~~OFFICIAL USE ONLY~~

The facilities of Argonne National Laboratory are owned by the United States Government. Under the terms of a contract (W-31-109-Eng-38) among the U. S. Department of Energy, Argonne Universities Association and The University of Chicago, the University employs the staff and operates the Laboratory in accordance with policies and programs formulated, approved and reviewed by the Association.

MEMBERS OF ARGONNE UNIVERSITIES ASSOCIATION

The University of Arizona
Carnegie-Mellon University
Case Western Reserve University
The University of Chicago
University of Cincinnati
Illinois Institute of Technology
University of Illinois
Indiana University
The University of Iowa
Iowa State University
The University of Kansas
Kansas State University
Loyola University of Chicago
Marquette University
The University of Michigan
Michigan State University
University of Minnesota
University of Missouri
Northwestern University
University of Notre Dame
The Ohio State University
Ohio University
The Pennsylvania State University
Purdue University
Saint Louis University
Southern Illinois University
The University of Texas at Austin
Washington University
Wayne State University
The University of Wisconsin-Madison

NOTICE

This report was prepared as an account of work sponsored by an agency of the United States Government. Neither the United States Government or any agency thereof, nor any of their employees, make any warranty, express or implied, or assume any legal liability or responsibility for the accuracy, completeness, or usefulness of any information, apparatus, product, or process disclosed, or represent that its use would not infringe privately owned rights. Reference herein to any specific commercial product, process, or service by trade name, mark, manufacturer, or otherwise, does not necessarily constitute or imply its endorsement, recommendation, or favoring by the United States Government or any agency thereof. The views and opinions of authors expressed herein do not necessarily state or reflect those of the United States Government or any agency thereof.

Printed in the United States of America
Available from
U. S. Department of Energy
Technical Information Center
P. O. Box 62
Oak Ridge, Tennessee 37830
Price: Printed Copy $4.50

~~OFFICIAL USE ONLY~~

DISCLAIMER

This report was prepared as an account of work sponsored by an agency of the United States Government. Neither the United States Government nor any agency Thereof, nor any of their employees, makes any warranty, express or implied, or assumes any legal liability or responsibility for the accuracy, completeness, or usefulness of any information, apparatus, product, or process disclosed, or represents that its use would not infringe privately owned rights. Reference herein to any specific commercial product, process, or service by trade name, trademark, manufacturer, or otherwise does not necessarily constitute or imply its endorsement, recommendation, or favoring by the United States Government or any agency thereof. The views and opinions of authors expressed herein do not necessarily state or reflect those of the United States Government or any agency thereof.

DISCLAIMER

Portions of this document may be illegible in electronic image products. Images are produced from the best available original document.

Distribution Category:
Consolidated Fuel Reprocessing
Program (UC-86)

ANL-80-15

ARGONNE NATIONAL LABORATORY
9700 South Cass Avenue
Argonne, Illinois 60439

DEVELOPMENT OF A 25-CM ANNULAR CENTRIFUGAL CONTACTOR

by

R. A. Leonard, G. J. Bernstein,
and A. A. Ziegler

Chemical Engineering Division

~~APPLIED TECHNOLOGY~~

~~Any Further Distribution by any Holder of this Document or of Other Data Therein to Third Parties Representing Foreign Interests, Foreign Governments, Foreign Companies and Foreign Subsidiaries or Foreign Divisions of U. S. Companies Should Be Coordinated with the Director, Division of Nuclear Fuel Cycle, Department of Energy. (U83-86)~~

June 1980

DISCLAIMER

This report was prepared as an account of work sponsored by an agency of the United States Government. Neither the United States Government nor any agency thereof, nor any of their employees, makes any warranty, express or implied, or assumes any legal liability or responsibility for the accuracy, completeness, or usefulness of any information, apparatus, product, or process disclosed, or represents that its use would not infringe privately owned rights. Reference herein to any specific commercial product, process, or service by trade name, trademark, manufacturer, or otherwise does not necessarily constitute or imply its endorsement, recommendation, or favoring by the United States Government or any agency thereof. The views and opinions of authors expressed herein do not necessarily state or reflect those of the United States Government or any agency thereof.

~~RELEASED FOR ANNOUNCEMENT IN ALDR.~~
~~Distribution limited to participants in the Consolidated Fuel Reprocessing Program.~~
~~Others request from Program Mgr. CFRP, OROO.~~

~~OFFICIAL USE ONLY~~

~~OFFICIAL USE ONLY~~

TABLE OF CONTENTS

	Page
ABSTRACT	1
I. INTRODUCTION	1
II. THEORY	2
III. CONTACTOR DESIGN AND MECHANICS	4
A. Important Design Features	4
B. Rotor Balance	6
IV. HYDRAULIC FLOW AND DISPERSION TESTS	13
A. Liquid Rise over Weirs	15
B. Gravity Dispersion Numbers	16
C. Dispersion-Band Model	18
D. Liquid Height in the Couette Mixing Zone	23
E. Contactor Capacity	25
V. MIXING POWER	27
VI. DISCUSSION	30
ACKNOWLEDGMENTS	30
REFERENCES	31

~~OFFICIAL USE ONLY~~

LIST OF FIGURES

No.	Title	Page
1.	Schematic of the Annular Centrifugal Contactor	3
2.	Overall View of 25-cm Contactor	5
3.	Partially Assembled Contactor Rotor	6
4.	Contactor Housing during Fabrication	7
5.	Rotor Shaft Connection to Motorized Spindle	10
6.	Profile of Vibrational Velocities for the Empty Well-Balanced 25-cm Rotor	11
7.	Profile of Vibrational Velocities for the Full Well-Balanced 25-cm Rotor	12
8.	Effect of Liquid Volume in the 25-cm-dia Rotor on the Vibrational-Velocity Profile	13
9.	Effect of Weight Added to the Full Well-Balanced Rotor on the Rotor Speed at Constant Vibrational Velocity	14
10.	Effect of Flow Rate on Liquid Rise over the Organic Weir	16
11.	Effect of Flow Rate on Liquid Rise over the Aqueous Weir	17
12.	Effect of Flow Rate on Acceptable Weir Pressure for Aqueous-Continuous Operation	19
13.	Effect of Flow Rate on Acceptable Weir Pressure for Organic-Continuous Operation of 25-cm Contactor at 1200 rpm, O/A = 1.0	20
14.	Effect of Flow Rate on Acceptable Weir Pressure for Organic-Continuous Operation of 25-cm Contactor at 1200 rpm, O/A = 5.0	21
15.	Effect of Flow Rate on Acceptable Weir Pressure for Organic-Continuous Operation of 25-cm Contactor at 1450 rpm, O/A = 1.0	22
16.	Effect of Flow Rate and Rotor Speed on the Liquid Level in the Couette Mixing Zone	23

~~OFFICIAL USE ONLY~~

LIST OF FIGURES (contd)

No.	Title	Page
17.	Effect of Rotor Speed on 25-cm Contactor Capacity	25
18.	Effect of Rotor Speed on Aqueous Weir Pressure for Various 25-cm Contactor Capacities	26
19.	Correlation of Mixing Power with the Operating Parameters of the 25-cm Contactor	28

~~OFFICIAL USE ONLY~~

LIST OF TABLES

No.	Title	Page
1.	Rotor Design	8
2.	Housing Design	9
3.	Test Liquids	14
4.	Gravity N_{Di} Values	18
5.	Contactor Power Requirements	29

~~OFFICIAL USE ONLY~~

DEVELOPMENT OF A 25-CM ANNULAR CENTRIFUGAL CONTACTOR

by

R. A. Leonard, G. J. Bernstein, and A. A. Ziegler

ABSTRACT

A large annular centrifugal contactor with a 25-cm-dia rotor has been developed and tested for hydraulic performance. It has a demonstrated capacity of 120 L/min which, with some changes, could be increased to 170 L/min. Thus, the contactor should be adequate for the A-Bank of a nuclear fuel reprocessing plant (10 Mg/d of heavy metal) based on the Purex flowsheet where flow rates reach 114 L/min (30 gal/min).

Detailed measurements made during the tests include rotor vibration levels, the liquid rise over the rotor weirs, the effect of organic-to-aqueous ratio on operation, and mixing power requirements. When the dimensionless dispersion number is measured and combined with the correlation for liquid rise over the circular weirs, the operating characteristics of the centrifugal contactor can be calculated.

I. INTRODUCTION

The development of a 10-Mg/d annular centrifugal contactor for the aqueous reprocessing of light-water reactor (LWR) spent nuclear fuel by solvent extraction was undertaken as part of a larger program on LWR fuel recyle being carried out at Savannah River Laboratory (SRL). The scope of the overall program is detailed elsewhere [RANEY]. The annular centrifugal contactor is an ANL modification [BERNSTEIN] of the earlier SRL design [KISHBAUGH] [WEBSTER] such that the paddle mixer of the SRL contactor is replaced by mixing the liquids in the annular (Couette) region between the centrifugal rotor and its stationary housing. The ANL modified contactor retains the advantages of the SRL contactor such as high capacity, short residence time to minimize solvent degradation, and improved criticality safety. In addition, the ANL contactor has greater ease of remote maintenance and a simpler design which lowers fabrication costs.

In addition to the effort on the large 10-Mg/d contactor which has a 25-cm-dia rotor, other work is being carried out at ANL with smaller centrifugal contactors. The development of the 0.5-Mg/d contactor is continuing with extensive testing of units with 9- and 12-cm-dia rotors. Development of a miniature annular centrifugal contactor with 2-cm-dia rotors has been completed [LEONARD-A]. The multistage miniature contactor can be used to evaluate potential flowsheets on a laboratory scale.

In this report, the development of a 10-Mg/d contactor is described in four sections. First, a qualitative description of contactor operation is

~~OFFICIAL USE ONLY~~

given. Second, contactor design and mechanics are discussed from fabrication through a check of contactor vibration. Third, the hydraulic flow and dispersion tests are presented using the correlations, models, and dimensionless dispersion number that were developed during the testing of the smaller contactors. Fourth, contactor mixing power is measured and correlated with operating parameters. To complete the contactor tests, the mass-transfer efficiency of uranium should be measured under Purex process conditions. Based upon the results of earlier tests at ANL using the smaller annular centrifugal contactors, extraction efficiency is expected to be greater than 98%.

II. THEORY

Contactor operation may be qualitatively followed using the schematic shown in Fig. 1. The immiscible phases flow into the Couette mixing zone which is the annular region between the spinning rotor and the stationary housing. The more dense phase is typically an aqueous phase and the less dense phase is typically an organic phase so that the terms aqueous and organic used throughout this report mean, in a more general sense, the more dense phase and the less dense phase, respectively. The liquid-liquid dispersion formed in the Couette mixing zone flows by gravity to the rotor inlet at the bottom of the rotor and thus into the centrifugal separating zone within the rotor. Here, the dispersion breaks rapidly under the centrifugal force. The separated phases flow over their respective weirs and are thrown from the rotor into their respective collector rings in the housing. Each liquid leaves its collector ring through a tangential exit port. A multistage countercurrent solvent-extraction system can be constructed by connecting a number of individual contactors in series.

A number of specific design features are required to ensure good contactor operation. The annular gap between the rotor and housing must be large enough to minimize resistance to downward flow, but not so large as to cause excessive holdup. Stationary radial vanes must be attached to the housing below and close to the rotor to dissipate the rotational velocity of the dispersion and allow it to flow inward to the rotor inlet orifice. The rotor orifice must be large enough to minimize resistance to flow into the rotor but must be sufficiently smaller than the organic-phase overflow weir to cause liquids to be pumped up through the rotor. Axial vanes in the rotor are necessary to ensure that the liquids will rotate with the same angular velocity as the rotor. A diverter disk is located in the rotor just above the inlet to direct the entering dispersion to approximately the median radial distance. Air vents must be provided near the center of the disk to permit the passage of air entrained in the dispersion. A specific feature, developed at SRL, is an air-controlled aqueous weir which employs air pressure to control the position of the dispersion band in the separating zone. This band is the zone of uncoalesced dispersion which lies between the organic (less-dense phase) weir and the aqueous (more-dense phase) underflow.

Using the concept of a dispersion band, the operation of the contactor can be made clearer. The shape and location of this band is that of a vertical thick-walled tube in the separating zone of the rotor. At a given rotor speed,

~~OFFICIAL USE ONLY~~

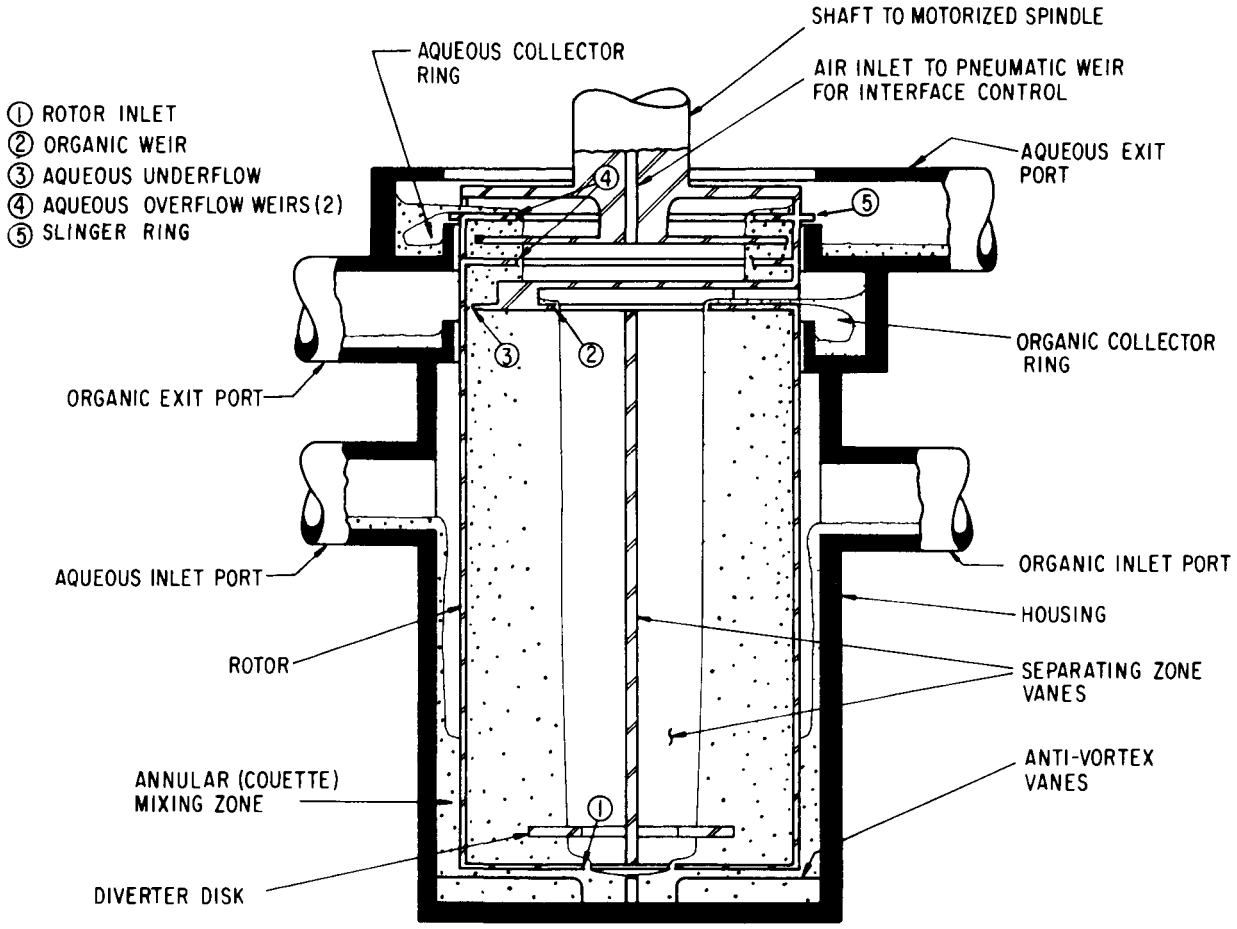

Fig. 1. Schematic of the Annular Centrifugal Contactor

dispersion-band thickness increases as throughput increases. The aqueous weir pressure is adjusted to keep the dispersion band in the separating zone. If the pressure is too high, the dispersion band reaches the organic weir and aqueous phase appears in the organic exit stream. If the pressure is too low, the dispersion band reaches the aqueous underflow and organic phase appears in the aqueous exit stream. At maximum throughput, only one aqueous weir pressure is acceptable. At this pressure, the dispersion band reaches from the organic

~~OFFICIAL USE ONLY~~

weir to the aqueous underflow and any further increase in flow will result in the appearance of both organic phase in the aqueous exit stream and aqueous phase in the organic exit stream.

III. CONTACTOR DESIGN AND MECHANICS

A. Important Design Features

An overall view of the assembled 25-cm* contactor and the 3.73-kW (5-hp) Whitnon motorized spindle that drives it are shown in Fig. 2. In Fig. 3, the contactor rotor is shown during fabrication before the outer sleeve was welded in place. This photograph shows the internal vanes, the weirs, the aqueous underflow, the inlet and exit ports, and the diverter disk. A third photograph, Fig. 4, shows the tangential exit ports and the collector rings of the contactor housing. For the rotor to use these exit ports effectively, the rotor must turn in a counterclockwise direction when viewed from below. Details of the 25-cm contactor are available in ANL shop drawings (CE-D7047 and CE-D7047A). Important contactor dimensions are included in Tables 1 and 2 for the rotor and housing, respectively.

Connection of the rotor to the motorized spindle is accomplished using a tapered rotor shaft which is inserted into the spindle as shown in Fig. 5. Pertinent motorized spindle dimensions are included in Table 1. In particular, the shaft, as it emerges from the nose of the motorized spindle, has a diameter of 57.2 mm (2.25 in.). Before the rotor shaft and the spindle sleeve are joined, both surfaces must be wiped clean and coated with a very light oil which does not form a continuous film. Then the rotor shaft is forced up sharply into the spindle nose. This connection must be tight so that the rotor is held firmly in place during operation. The rotor is further secured with a hollow draw bar which goes down through the hollow shaft of the motorized spindle to the rotor shaft. The draw bar is screwed (left-handed threads) into the end of the rotor shaft and tightened to a torque of 27 N·m (20 ft-lb). At the top end of this hollow draw bar, a rotary union (Deublin Co., Northbrook, IL.) is attached so that a controlled air pressure can be supplied over the inner aqueous weir.

The motorized spindle is mounted on one side of a channel-iron frame which is 787-mm high and 406-mm wide. This frame rests on and is bolted to a 686-mm-square heavy steel plate that is 38-mm thick. The contactor housing is bolted to this horizontal plate from below. The channel-iron frame is further braced by two triangular steel plates which are perpendicular to the plane of the frame and extend down to the heavy horizontal plate. These triangular plates can be seen in Fig. 1. Vibrations in this channel-iron frame, especially in the plane of the frame, were excessive [greater than 2.5 mm/s (0.1 in./s) as will be discussed further below] and had to be controlled by clamping the upper frame to angle irons which were secured to nearby steel beams. Thus, the frame to which the motorized spindle is mounted should be redesigned as a part of future development work.

---

*For convenience, a contactor is described in terms of the nominal diameter of its rotor; thus a "25-cm contactor" is a contactor having a 25-cm-dia rotor.

OFFICIAL USE ONLY

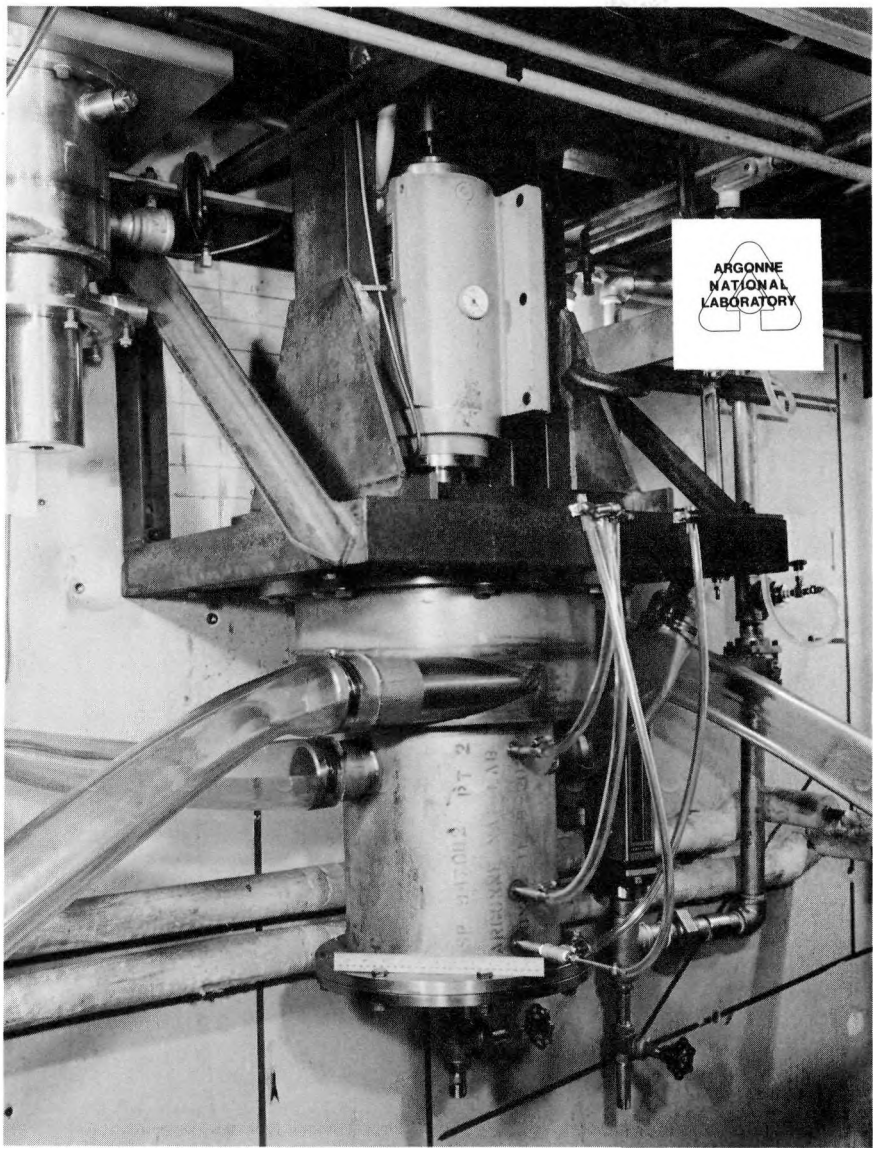

Fig. 2. Overall View of 25-cm Contactor.
ANL Neg. No. 308-79-649.

Originally, the vanes in the separating zone of the rotor were welded only at the top and bottom, i.e. to the organic weir plate and the rotor inlet-orifice plate, respectively. Later, in an effort to improve dynamic balance by increasing the stiffness of the rotor, the vanes were also welded to the side wall of the rotor. However, this change had no effect upon the dynamic balance and the maximum acceptable rotor speed was unchanged.

~~OFFICIAL USE ONLY~~

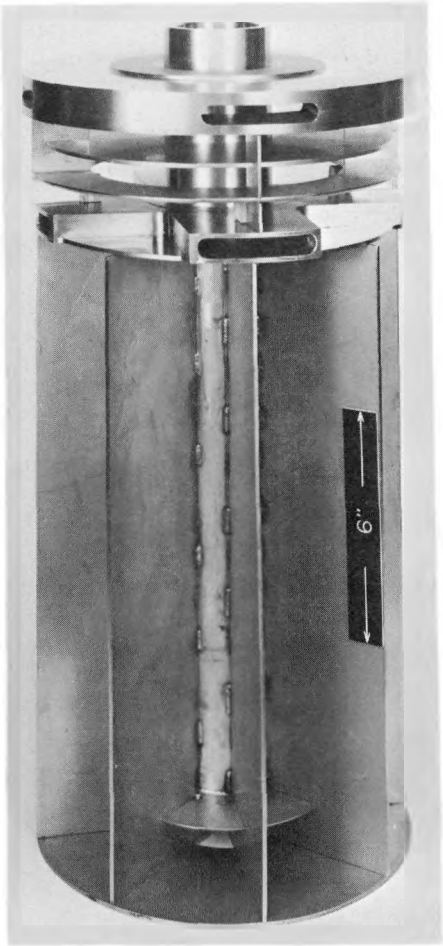

Fig. 3. Partially Assembled Contactor Rotor.
ANL Neg. No. 308-78-678.

B. Rotor Balance

To prevent undue wear on the bearings in the motorized spindle, additional metal was removed from the rotor so that it had good starting (static) balance and good running balance. Since balance can always be attained by adding (or removing) two weights placed in different arbitrarily chosen planes perpendicular to the rotor axis [BRAND], the standing balance was obtained mainly by removing metal from the heavy slinger ring at the top of the rotor. This was done by drilling blind holes between the aqueous exit ports. The final standing balance and the running balance were obtained by removing some additional metal from the rotor wall at the bottom of the rotor.

~~OFFICIAL USE ONLY~~

Fig. 4. Contactor Housing during Fabrication (Collector-Ring Zone). ANL Neg. No. 308-78-681.

In order to balance the rotor, one must be able to vary the motor speed, measure the level of vibration, and attach weights. A variable-frequency generator was used to vary the rotor speed from 550 to 2750 rpm. The vibrational velocity was measured with a Vibropac I vibration meter (Model 675, Balance Technology, Inc., Ann Arbor MI 48103). Readings were made with the pickup mounted on the motorized spindle housing just over the lower bearings. A heavy white tape was used to add weight at the desired location on the rotor. If several layers of tape were required, the tape was further secured to the rotor by strapping tape with a 360-, 720-, or 1080°- wrap around the rotor. When the proper location and mass of the tape were established, equivalent metal was removed from the rotor at the same axial location but on the opposite side of the rotor from the tape.

Rotor balance was measured by increasing the rotor speed incrementally from 550 rpm up to some speed where the vibrational velocity approaches 2.5 mm/s (0.1 in./s). In the Vibropac instruction manual, this is the suggested upper vibrational velocity limit for smooth, no-fault operation of machinery. As rotor balance is improved, the rotor speed required to reach this limiting vibrational velocity increases. In later tests, the rotor speed was measured only at vibrational velocities of 0.9 mm/s (0.035 in./s), 1.4 mm/s (0.055 in./s), and 2.0 mm/s (0.08 in./s). The limiting rotor speed is determined by extrapolating the data to 2.5 mm/s (0.1 in./s) and noting the rotor speed required to reach this vibrational velocity.

~~OFFICIAL USE ONLY~~

Table 1. Rotor Design

Design parameter	Specification
Nominal diameter, cm (in.)	25[a](10)
Actual average diameter, mm	262
Pertinent ANL drawings	CE-D7047A
Rotor outside diameter, mm	264.9[b]
Rotor inside diameter, mm	257.2
Rotor inlet diameter, mm	76.2
Separating-zone length, mm	414.3
No. of separating-zone vanes	8[c]
Dispersion disk	Yes[d]
Organic weir radius, mm	50.8
Organic weir thickness, mm	3.2
Aqueous underflow radius, mm	122.4
Width of the riser gap up to aqueous weir, mm	19.0
No. of vanes in riser gap up to aqueous weir	4
Riser vanes flush with aqueous weir	Yes
Aqueous weir radius, mm	88.7[e]
Aqueous weir thickness, mm	3.2
Height of aqueous weir above organic weir, mm	38.1
Clearance between aqueous weir and center shaft, mm	50.8
Separating-zone vanes flush with organic weir	Yes[c]
Slinger ring[f] diameter, mm	279.4
Length of rotor below slinger ring, mm	503.2
Total rotor length excluding tapered shaft, mm	576.3
Total tapered shaft length, mm	241.3
Length of tapered shaft outside the motorized spindle, mm	12.4
Tapered shaft diameter where it enters the nose of the motorized spindle, mm	57.2
Taper on shaft into the motorized spindle, mm/mm	0.05
Distance from the midpoint of the lower bearings of the motorized spindle to its nose, mm	182[g]
Outside diameter of the central spindle shaft at the lower bearings, mm	76.2[g]
Outside diameter of the central spindle shaft below the main housing of the spindle, mm	95.3[g]
Length of the motorized spindle shaft below the main housing of the spindle, mm	136.5[g]
Length of the straight shaft and shoulder from top of rotor to the tapered shaft, mm	42.9
Outside diameter of the straight shaft just above the rotor, mm	76.2
Rotor weight, kg	44.3
Rotor material	304 stainless steel

[a]This value follows from the original designation of this rotor as a nominal 10-in.-dia rotor.

[b]Actual value. Drawing shows 266.7 mm.

[c]These axial vanes extend out radially to the rotor wall from center tube which has an O.D. of 63.5 mm and a wall thickness of 6.4 mm. The vane thickness is 2.4 mm. The center tube stops at the dispersion disk. In the 28.6-mm distance below this, from the dispersion disk to the rotor inlet orifice plate, the vanes extend out radially to the rotor wall from the axis of the rotor. For the 12.7 mm just below the organic weir, the vanes are notched 19.0 mm so that the vanes extend in radially only to the edge of the organic weir from the rotor wall.

[d]This disk has a 152.4-mm diameter and is 3.2-mm thick. It has eight vent holes of 6.4-mm diameter located on an 81.0-mm-dia bolt circle.

[e]Drawing called for 88.9 ± 0.2 mm. Measured value using calipers is 88.4 ± 0.3 mm. The 88.7-mm value listed here and used to make various calculations represents the best average value for aqueous weir radius, r_{*a}.

[f]The slinger ring of the rotor rides just above the lip of the aqueous collector ring.

[g]Dimension taken from Whitnon Spindle Division (Mite Corp., Farmington, Conn.) Print No. 642-1880-07-0 entitled "Base Mounted Motorized Spindle, 1800 rpm, Grease Lube SRI #2" and dated 4-21-77.

~~OFFICIAL USE ONLY~~

Table 2. Housing Design

Design parameter	Specification
Pertinent ANL drawings	CE-D7047
Inside diameter of the housing at the mixing zone (outside diameter of the mixing zone), mm	312[a]
Couette mixing gap, mm	23.6
Mixing-zone length, mm	366.6
Rotor length in mixing zone, mm	348.4
Bottom radial vane height, mm	17.5
No. of bottom radial vanes	8
Vane thickness, mm	3.2
Rotor-to-vane gap, mm	0.8
Inlet lines perpendicular to housing	Yes
Height of inlet centerline above the bottom of the rotor, mm	280.2
Height of organic collector ring lip above the bottom of the rotor, mm	411.9
Outlet lines tangential to housing	Yes
Inside diameter of ports, mm	77.9
Minimum inside diameter (at collector rings), mm	273.0
Rotor-to-housing gap at the collector ring, mm	4.0
Height of aqueous collector ring lip above the bottom of the rotor, mm	499.3
Width of collector ring channels, mm	80.2
Height of collector ring lip, mm	50.8
Height of organic collector ring channel, mm	81.0
Height of aqueous collector ring channel, mm	95.2
Height of slinger ring above the lip of the aqueous collector ring, mm	3.9
Housing material	304 Stainless Steel

[a]Actual value. Drawing shows 304.8 mm.

The results of balancing the empty rotor are shown in Fig. 6, along with the rotor balance before final balancing was started. These results indicate the rotor can be operated at up to 1870 rpm. The dashed lines on either side of the best-balance curve show the trade-offs that must be made when balancing the rotor. One side gives lower vibrational velocities at lower rotor speeds but also shows that the 2.5-mm/s limit is reached at a lower rotor speed. The other side gives higher vibrational velocities at lower rotor speeds but also shows the rotor can be operated at a higher speed before reaching the 2.5-mm/s limit. The graph shows that this balancing technique is sensitive to changes of mass of less than 3 g (1.1 oz) at the surface of the rotor.

In a similar fashion, the balance was checked with the rotor full of water. The results, seen in Fig. 7, show the final approach to 2.5 mm/s

~~OFFICIAL USE ONLY~~

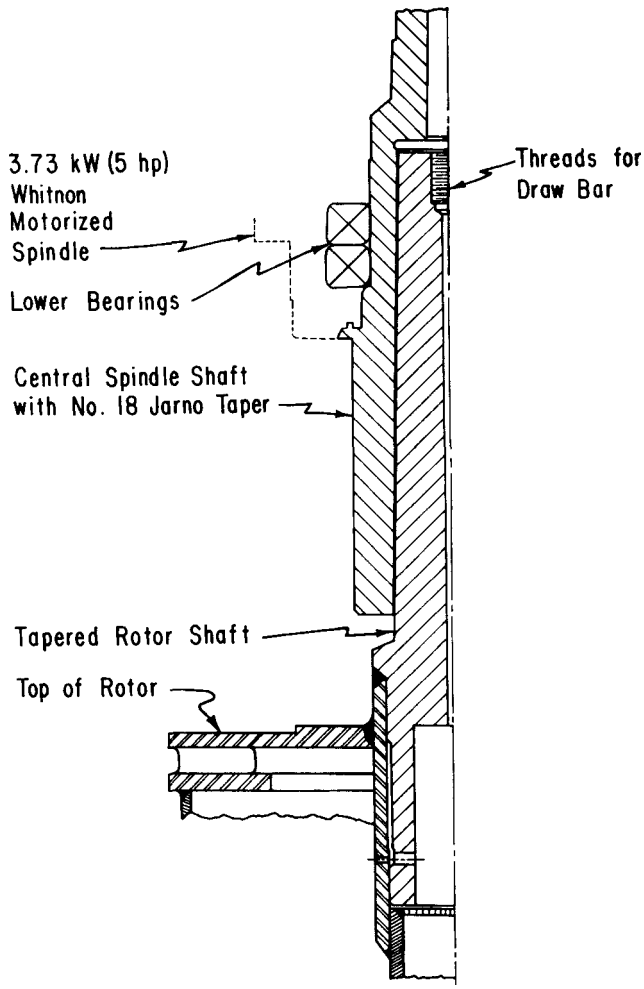

Fig. 5. Rotor Shaft Connection to Motorized Spindle.

(0.1 in./s) occurs at lower rotor speeds than with an empty rotor, so that the rotor under normal operating conditions (i.e., filled with liquid) can be operated only up to 1500 rpm. In practice, the rotor was operated at a maximum of 1450 rpm so that the vibrational velocity was only 1.3 mm/s (0.055 in./s). To get the water into the rotor without putting on the contactor housing, a tank with the desired volume of water was raised up from below the rotor. Vanes were placed at the bottom of the tank to dissipate the rotational velocity of the water and allow it to flow into the rotor.

When the rotor had only a small amount of water in it (less than 4.4 L) the rotor speed which gave a vibrational velcoity of 2.5 mm/s (0.1 in./s) decreased as shown in Fig. 8. This was attributed to the presence of a steel rod (12.7 mm in diameter and 414 mm long) which was welded to the inside of

~~OFFICIAL USE ONLY~~

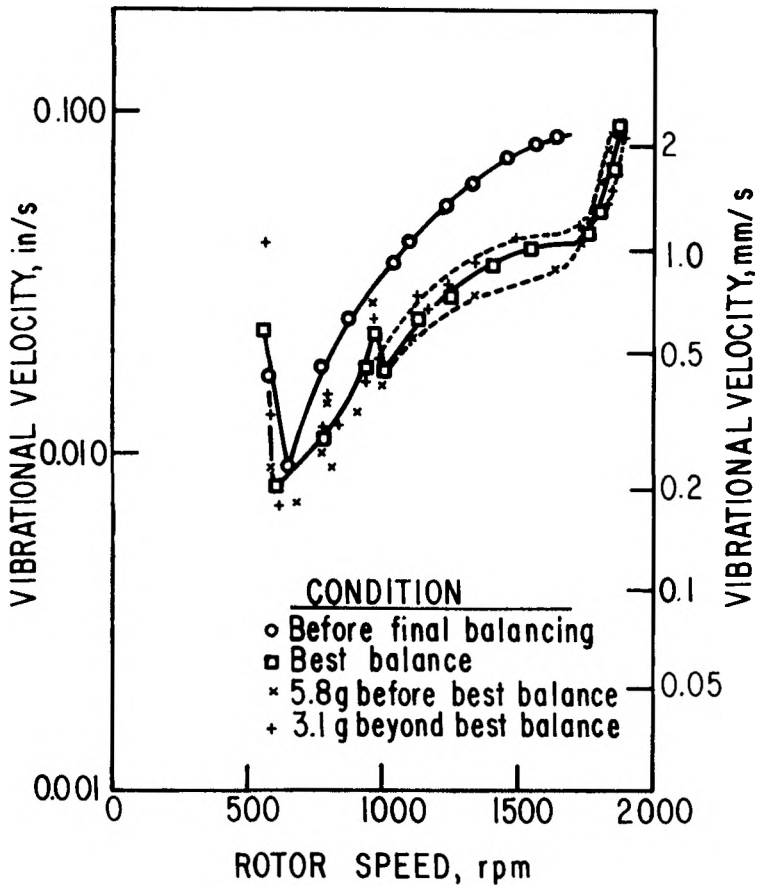

Fig. 6. Profile of Vibrational Velocities for the Empty Well-Balanced 25-cm Rotor

the rotor wall in the separating zone. This rod was added to put the rotor roughly in static balance before the final balancing with the rotor in the motorized spindle. The lack of rotor balance appeared to originate in the 10-in. stainless steel pipe from which the rotor was cut. Machining the pipe showed it was out-of-round and this could not be fully rectified by machining. Since the rod was rigid and more dense than the water, some unbalance occurred as enough water was added to partially submerge the rod. Such a rotor unbalance is seen in Fig. 8. This unbalance gradually disappeared as the rod was covered. When enough water was in the rotor to cover the rod, the rotor balance no longer changed.

Further effort was made to improve the balance of the rotor when it was full of water. To do this, weight was added to the rotor at successive locations about its circumference at three planes normal to the rotor axis. Then the rotor speed which resulted in 1.3-mm/s (0.05-in./s) vibrational velocity was measured. The results, shown in Fig. 9, indicate tha the best balance for the rotor filled with water is essentially the same as that for the empty rotor. Thus, the conclusion reached above that the maximum acceptable rotor

~~OFFICIAL USE ONLY~~

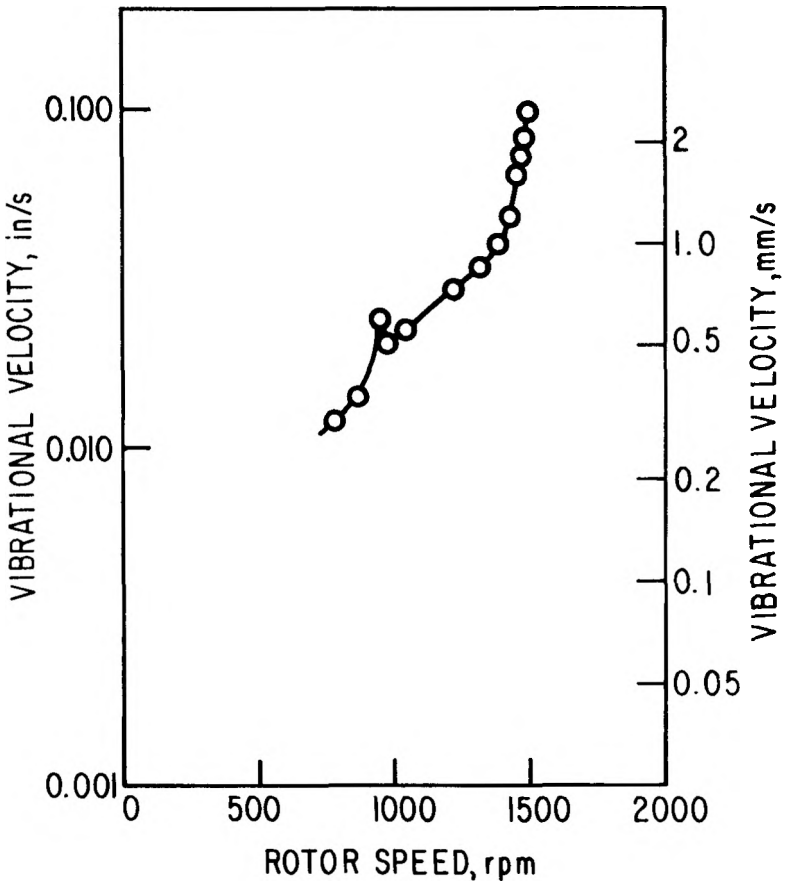

Fig. 7. Profile of Vibrational Velocities for the Full Well-Balanced 25-cm Rotor (>6L of Water).

speed is less when the rotor is filled with water, cannot be attributed to a difference in the balance required for the rotor when it is filled with water. The results also show that the rotor is much more sensitive to the position of the added weight about the rotor circumference than to the height of the weight above the bottom of the rotor.

The source of the vibrations which limit the rotor speed was not determined. This should be done in future contactor tests. If the source of the vibrations at 1500 rpm is from the mounting frame or the support plate, then stiffening of these structural members will allow contactor operation at higher rotational velocities. However, if the source of the vibrations is from a natural frequency (critical speed) of the rotating mass, then changes must be made to the motorized spindle rotor (e.g., using a larger motorized spindle) to the bearing stiffness in the motorized spindle, or to the contactor rotor (e.g., making the shaft from to contactor rotor to the motorized spindle thicker) in order to operate the contactor at higher rotational velocities.

~~OFFICIAL USE ONLY~~

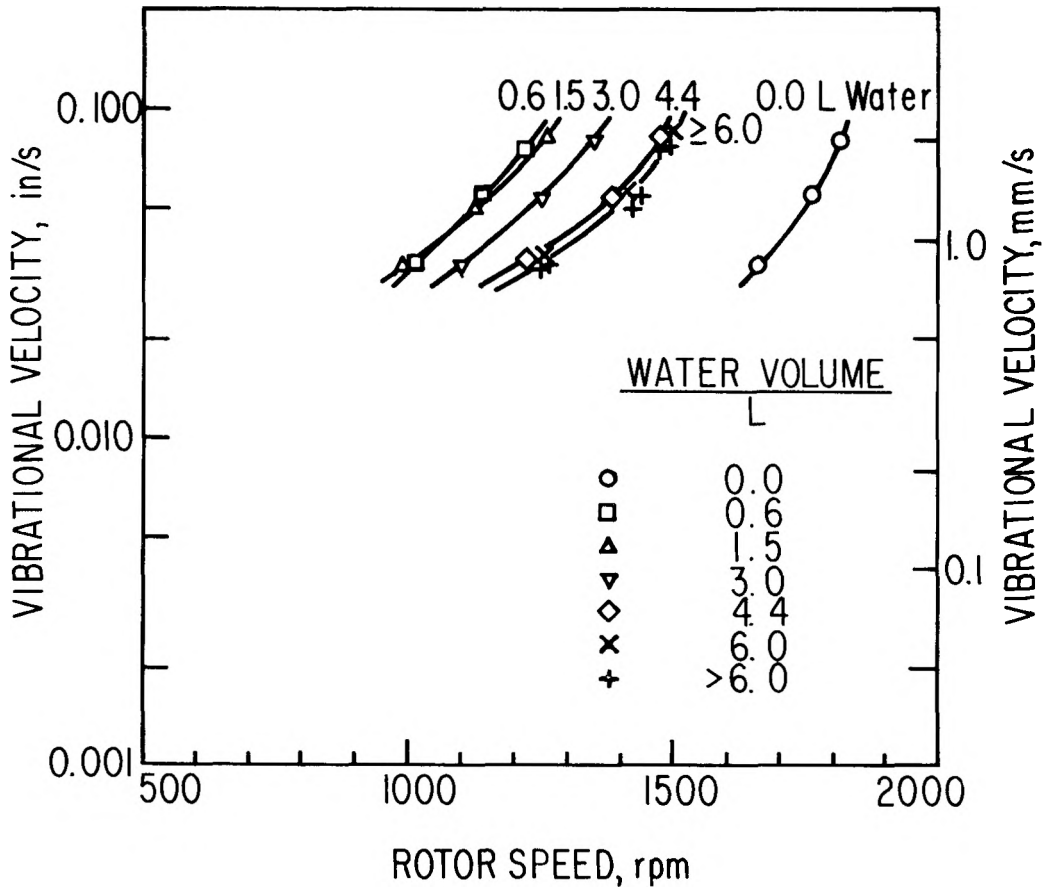

Fig. 8. Effect of Liquid Volume in the 25-cm-dia Rotor on the Vibrational-Velocity Profile.

Having a rotor that would run at 1800 rpm would eliminate the need for a variable-frequency generator and would also result in a proportional increase in contactor capacity.

When future rotors are built, the rotor wall should be rolled from flat, stainless steel sheet stock perhaps 2.4-mm (3/32-in.) thick, rather than machined from a stainless steel pipe. The final cylinder, after welding, would have the proper concentricity between the inner and outer walls which would minimize the effort required in final rotor balancing.

IV. HYDRAULIC FLOW AND DISPERSION TESTS

In this section, the hydraulic flow and dispersion tests are discussed in detail. These include measurement of the liquid rise over the circular weirs in the rotor, dispersion-number determinations, formulation of a quantitative model to predict dispersion-band location, a semi-theoretical correlation for liquid height in the Couette (annular) mixing zone, and the use of the dispersion number to predict contactor capacity. All tests were made with

~~OFFICIAL USE ONLY~~

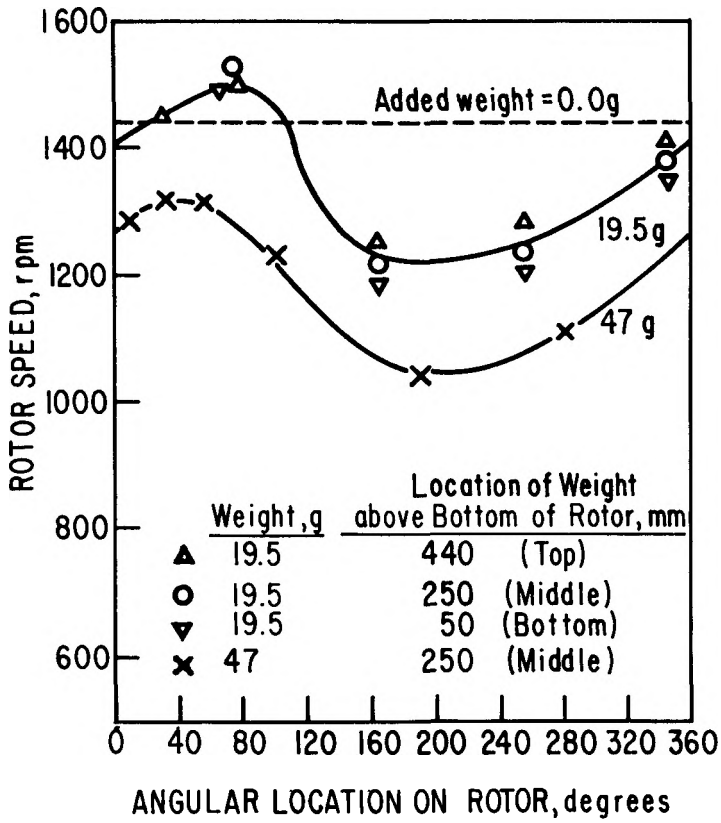

Fig. 9. Effect of Weight Added to the Full Well-Balanced Rotor on the Rotor Speed at Constant Vibrational Velocity. [Vibrational Velocity = 1.27 mm/s (0.05 in./s), >6 L of Water in 25-cm Rotor]

an aqueous phase of 0.3M HNO_3 and an organic phase of 30 vol % tributyl phosphate (TBP) in n-dodecane (nDD). Physical properties of these liquids are listed in Table 3.

Table 3. Test Liquids

Aqueous Phase (A): 0.3M HNO_3

Organic Phase (O): 30 vol % Tributyl Phosphate (TBP) in n-dodecane (nDD)

Phase	Density, kg/m^3	Viscosity, Pa·s
A	1008.3	0.001
O	826	.002

~~OFFICIAL USE ONLY~~

A. Liquid Rise over Weirs

Liquid rise over the circular weirs in the rotor was measured by a technique developed earlier [LEONARD-B]. The correlation presented there was checked and modified to fit the 25-cm-dia rotor. This modified correlation is part of the dispersion-band model presented below.

Flow over circular weirs in a centrifugal field is characterized by a weir coefficient k given by:

$$k = k_* \exp\left[-\left(\frac{4\theta}{bn}\right)(k_* f\pi)^{2/3}(q/\omega)^{1/3}\right] \tag{1}$$

where

b = vertical width of channel through which the liquid flows radially inward to reach the weir, m

f = fraction of the weir circumference available for flow, dimensionless

k_* = rectangular weir coefficient for a gravitational field, dimensionless

n = number of baffles just upstream of the weir, dimensionless

q = flow rate over the weir, m^3/s

θ = correlation factor for the effect of baffle extension over the weir, dimensionless

ω = angular velocity, rad/s

The θ term has been found to be 1.0 when the baffles just upstream of the weir extend to the center of the rotor. When the baffles stop at the weir, then the θ term has been found to be 0.333 in tests of a 9-cm contactor [LEONARD-B].

Both weirs were tested using the aqueous phase of 0.3M HNO_3 rather than the organic phase since the organic phase contained some dispersed aqueous phase which collected in the rotor and interfered with the test. Results for the organic and aqueous weirs are shown in Fig. 10 and 11, respectively. The curves show the predicted rise over the weir using Eq. 1 and various values of θ as indicated. For the organic weir, the Coriolis forces are low and the value of θ is not important. The organic weir test is sensitive to the aqueous weir radius giving experimental points that are all above the predicted curve if 88.4 mm is used and all below the curve if 88.9 mm is used. An aqueous weir radius of 88.7 mm was used for the experimental points shown in Fig. 10.

~~OFFICIAL USE ONLY~~

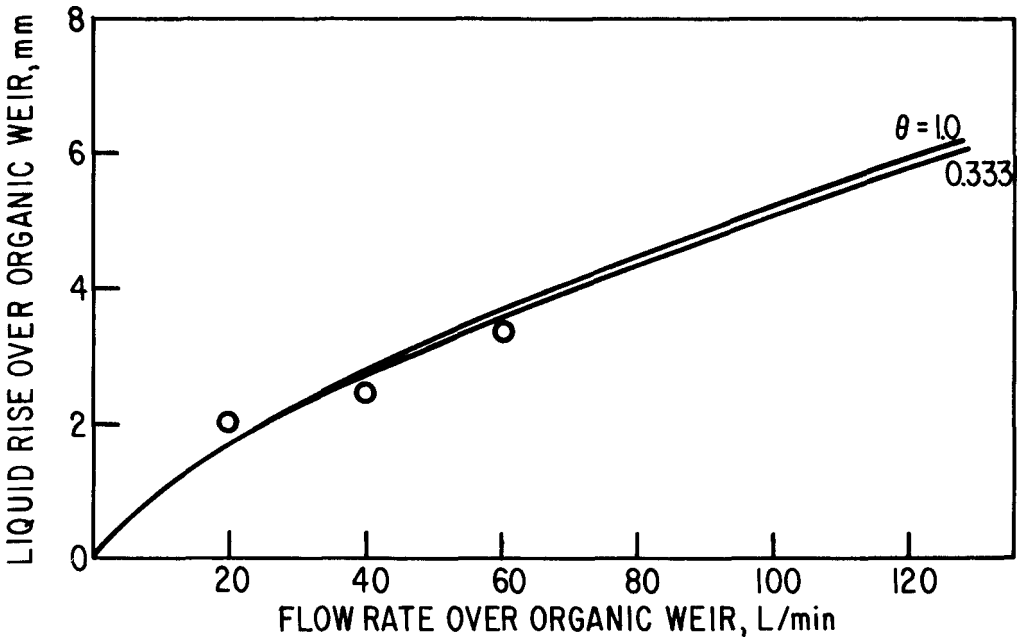

Fig. 10. Effect of Flow Rate on Liquid Rise over the Organic Weir. 25-cm-dia Rotor. Rotor Speed = 1200 rpm (125.7 rad/s). Density = 1008.2 kg/m^3. 0.3M HNO_3.

The results of these tests reinforce the choice of the 88.7-mm aqueous weir radius as specified in Table 1. With this aqueous weir radius, the data for the liquid rise over the aqueous weir were evaluated. For this weir, the Coriolis forces are significant and the θ value which best fits the experimental data is 0.667 rather than 0.333 which had been expected based on the 9-cm contactor tests.

B. Gravity Dispersion Numbers

The dimensionless dispersion number is measured for the dispersion in the Couette mixing zone by drawing off a sample of the dispersion. This sample, taken from just under the rotor, flows into a graduated cylinder where the time for the dispersion to break, t_B, under gravity, g, is measured for various dispersion heights, ΔZ. Then the dimensionless dispersion number, N_{Di}, is calculated from

$$N_{Di} = \frac{1}{t_B} \sqrt{\frac{\Delta Z}{g}} \qquad (2)$$

OFFICIAL USE ONLY

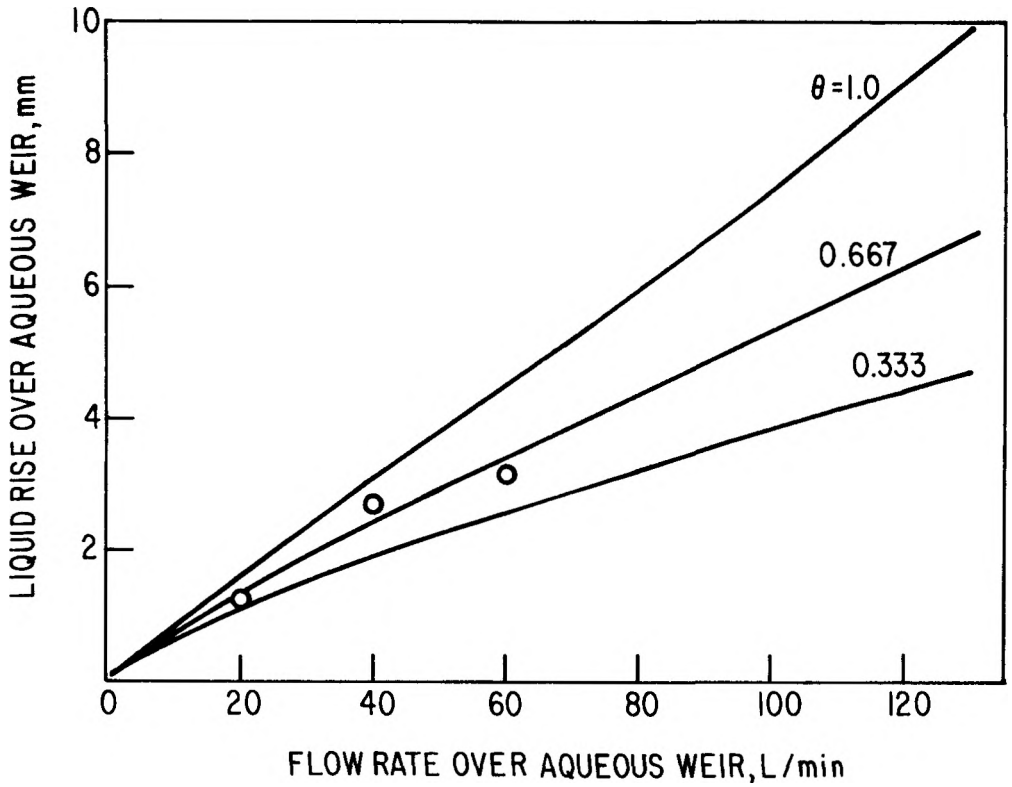

Fig. 11. Effect of Flow Rate on Liquid Rise over the Aqueous Weir. 25-cm-dia Rotor. Rotor Speed = 1200 rpm (125.7 rad/s). Density = 1008.2 kg/m^3. 0.3M HNO_3.

as given by [LEONARD-C]. The results, listed in Table 4, give an average N_{Di} of 1.01×10^{-3} for organic-continuous operation. The overall organic-to-aqueous (O/A) ratio of the feed streams and the O/A ratio of the dispersion taken from below the rotor are in good agreement. This agreement between O/A ratios indicates that one phase does not move through the mixing zone faster than the other phase.

Since the height of the dispersion in the graduate can be measured accurately and the gravitational acceleration is constant, the major source of error in determing N_{Di} is in measuring the time to break. At the high and low O/A ratios of 5 and 0.2, respectively, the time to break is difficult to estimate because a definite dispersion band either does not form or is very indistinct. Even when a layer with a high volume fraction (>0.75) of dispersed-phase as droplets does form next to the separated dispersed phase, some dispersed phase remains trapped in the continuous phase. Also, for operation at an O/A ratio of 5, the final two layers of dispersed-phase droplets, which are 2- to 4-mm thick, take much longer to break than the other layers.

~~OFFICIAL USE ONLY~~

These problems are not unexpected, since the range for a distinct dispersion band in a continuous gravity settler is between O/A values of 0.28 and 3.5 [BARNEA]. Thus, our high and low O/A values may be close to the limit of predictable operation.

Table 4. Gravity N_{Di} Values

Test conditions: 25-cm Contactor
Acceleration: 9.81 m/s^2
Settling lengths: 50, 100, 200, and 400 mm
A: 0.3M HNO_3
O: 30 vol % TBP in nDD

Rotor Speed, rpm (rad/s)	O/A	Range of Flow Rates, L/min	$N_{Di} \times 10^3$	Continuous Phase
600 (62.8)	1.0	50	0.92	O
900 (94.2)	1.0	80	.99	O
1200 (125.7)	0.2	54-80	2.9	A
1200 (125.7)	1.0	40-121	1.10	O
1200 (125.7)	5	40-70	1.00	O
1450 (151.8)	1.0	120	1.04	O

C. Dispersion-Band Model

A quantitative model for the dispersion band in the separating zone of the rotor has been worked out in two parts. First, a hydrostatic force balance locates the theoretical interface between the aqueous and organic phases in the rotor separating zone with the dispersion band completely coalesced. This balance includes many rotor dimensions, the density of both phases, the operating conditions including the air pressure over the inner aqueous weir, and the correlation which gives the liquid rise over the circular weirs. Second, the boundaries of the dispersion band relative to the theoretical interface are established by using the dimensionless dispersion number to find the volume of the dispersion band and the fraction of aqueous phase, ε, in the dispersion band. Normally ε is calculated by

$$\varepsilon = \frac{1}{1 + R} \tag{3}$$

where R is the ratio of organic phase to aqueous phase flowing to the contactor. That this form is appropriate has been demonstrated by [BARNEA] for gravity settlers. Since the calculations for this dispersion-band model are quite lengthy, they have been set up for a TI-59 programmable calculator as the PRACTICE (Pressure Range At Constant Throughput In Centrifugal Extractors) program and are reported in [LEONARD-D].

~~OFFICIAL USE ONLY~~

Experimental results are compared with theoretical predictions from the PRACTICE program in Figs. 12-15.

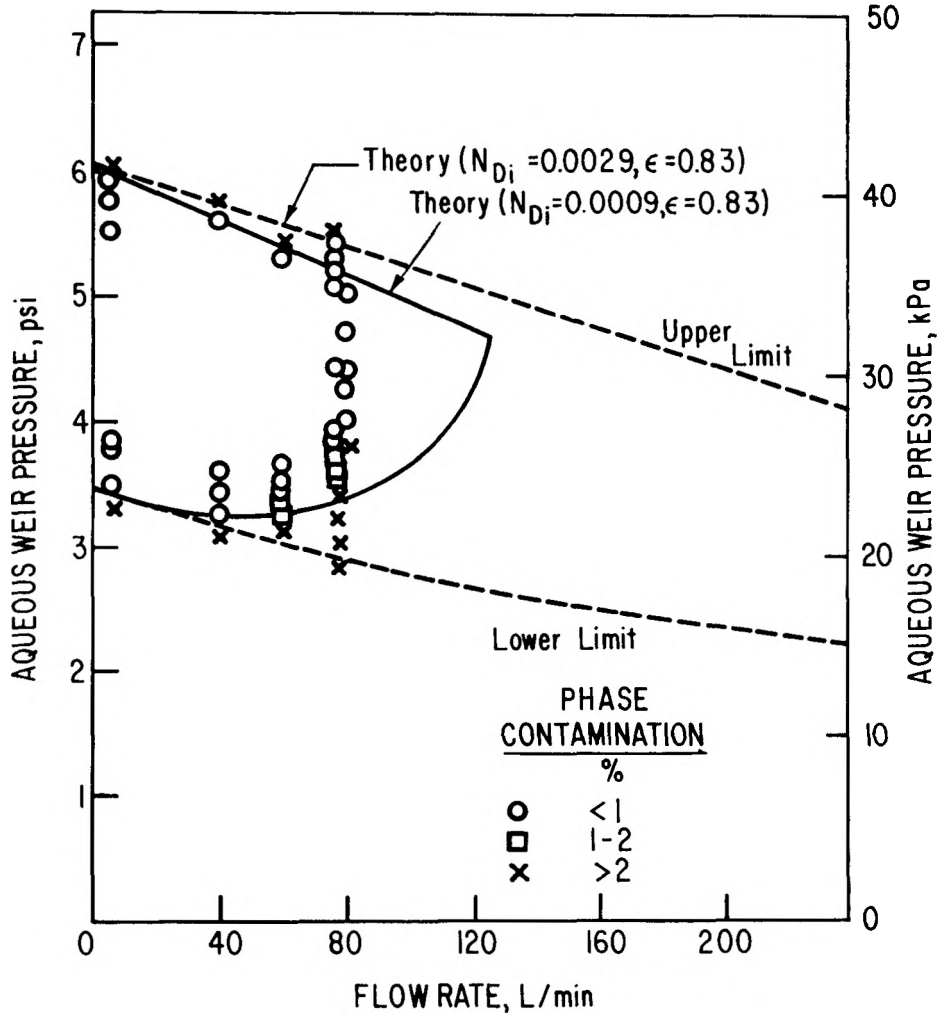

Fig. 12. Effect of Flow Rate on Acceptable Weir Pressure for Aqueous-Continuous Operation. [25-cm Contactor; Rotor Speed = 1200 rpm (125.7 rad/s); A: 0.3M HNO_3, O: 30% TBP in nDD, O/A = 0.2.]

Tests cover the O/A range from 0.2 to 5 and rotor speeds from 1200 to 1450 rpm. In general, there is reasonable agreement between theory and experiment. At O/A values of 1.0, throughput (total phases) of 120 L/min was demonstrated at 1200- and 1450-rpm rotor speeds. This throughput reflects the available capacity of the pumping system which was limited to about 60 L/min for each phase. For the same reason, at high and low O/A values of 5 and 0.2, respectively, throughput (total phases) was limited to less than 80 L/min. Theoretical predictions indicate contactor capacity should be considerably higher than 80 L/min.

~~OFFICIAL USE ONLY~~

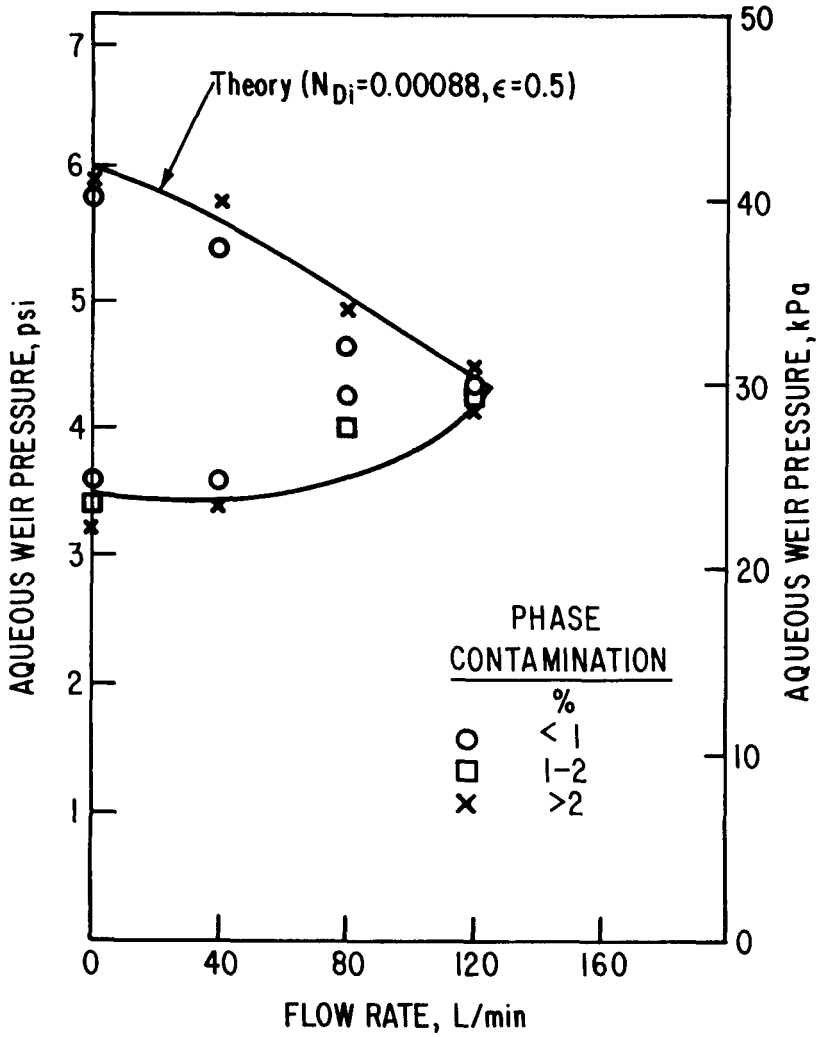

Fig. 13. Effect of Flow Rate on Acceptable Weir Pressure for Organic-Continuous Operation of 25-cm Contactor at 1200 rpm (125.7 rad/s), O/A = 1.0. (A: 0.3M HNO_3, O: 30% TBP in nDD)

Some further observations on the data in Figs. 12-15 can be made to verify the assumptions used in the development of the dispersion-band model. The value of the aqueous fraction required to fit the data at 1450 rpm in Fig. 15 is less (0.4 rather than 0.5) than predicted by Eq. 3. Otherwise, the aqueous fractions as calculated with Eq. 3 are in very good agreement with predicted values. For organic-continuous operation (Figs. 13-15) the average N_{Di} is 0.90×10^{-3} which agrees well with the N_{Di} of 1.01×10^{-3} determined under gravity conditions. The slight difference in values may represent the bias to stop measurement of the time to break before the final layer of droplets had broken. In further agreement, N_{Di} for the 2-cm contactor has been found to be 0.84×10^{-3} [LEONARD-A]. Tests on the 9- and 12-cm contactors also agree

OFFICIAL USE ONLY

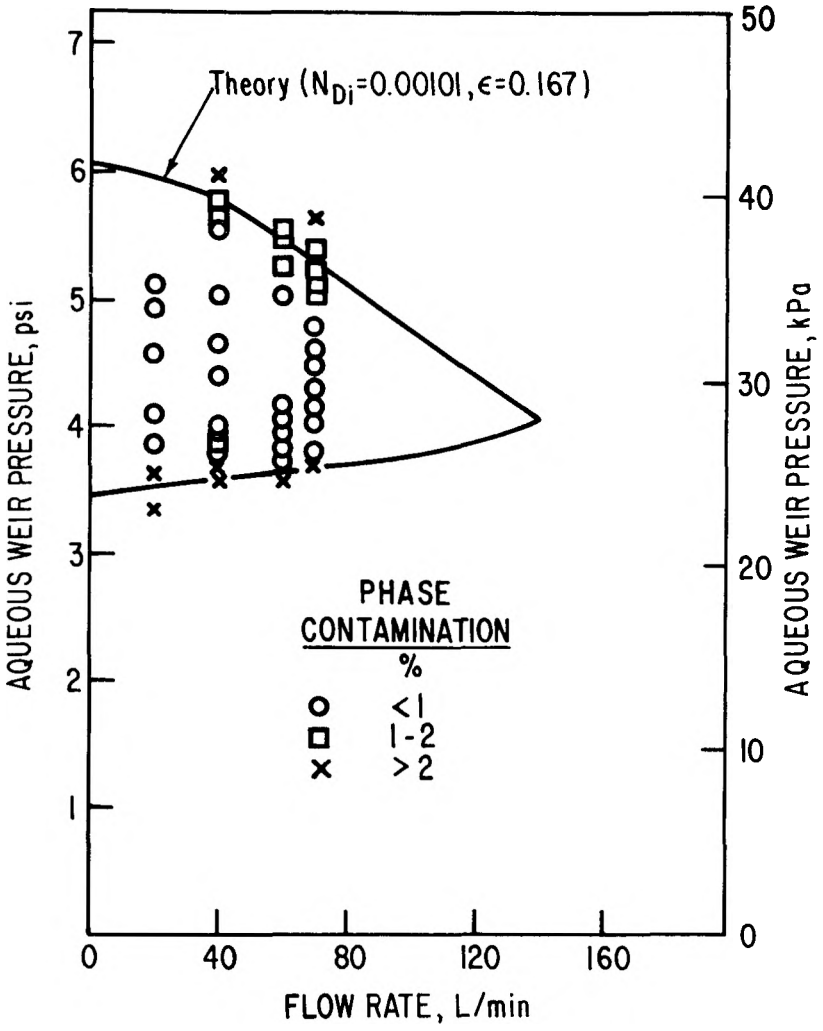

Fig. 14. Effect of Flow Rate on Acceptable Weir Pressure for Organic-Continuous Operation of 25-cm Contactor at 1200 rpm (125.7 rad/s), O/A = 5.0. (A: 0.3M HNO_3, O: 30% TBP in nDD)

with this range of N_{Di} values for organic-continuous operation. For aqueous-continuous operation (Fig. 12) the N_{Di} that fits the data best appears to be 0.90×10^{-3} even though the average gravity N_{Di} is 2.9×10^{-3}. Lack of pumping capacity prevented us from testing this apparent discrepancy at higher flow rates. However, as a conservative basis for design, when N_{Di} differs for the different continuous phases, the lower N_{Di} should be used.

In these tests, satisfactory operation is taken to be less than 1% phase contamination in both exiting streams and the liquid level in the lines feeding the Couette mixing zone must be below the organic collector ring. For the high and low O/A values of 5 and 0.2, respectively, the boundary between the

~~OFFICIAL USE ONLY~~

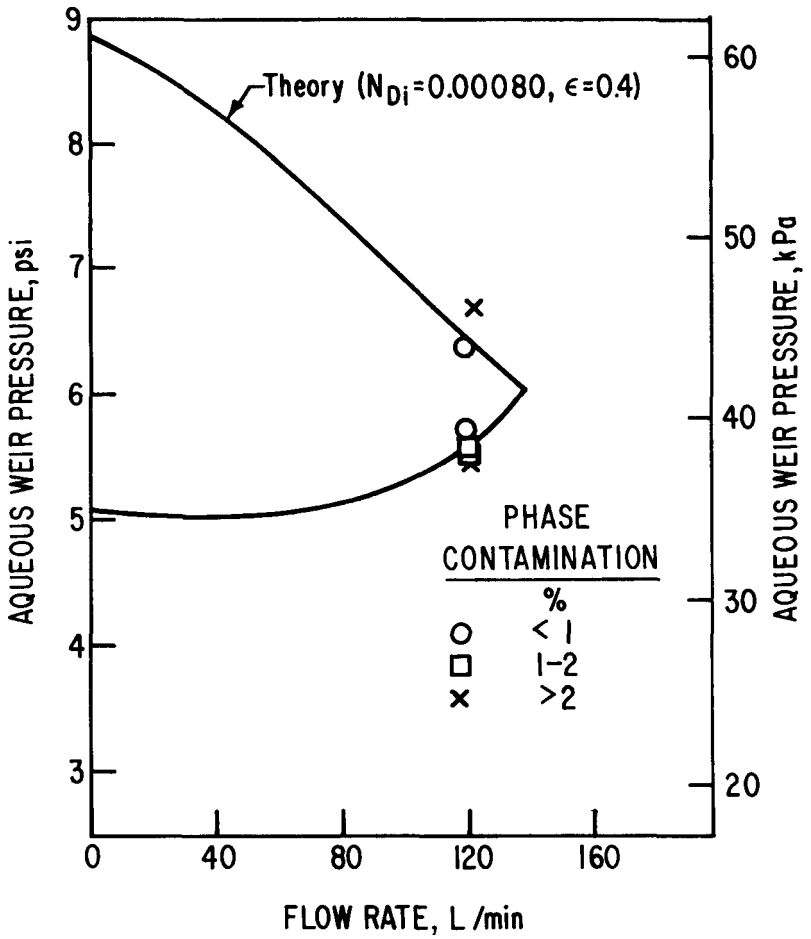

Fig. 15. Effect of Flow Rate on Acceptable Weir Pressure for Organic-Continuous Operation of 25-cm Contactor at 1450 rpm (151.8 rad/s), O/A = 1.0. (A: 0.3M HNO_3, O: 30% TBP in nDD)

separated continuous phase and the dispersion band is diffuse, so that the concentration of the dispersed phase increases more slowly as the dispersion band is shifted towards the continuous-phase exit. Because of this, the experimental data near the lower curve of Fig. 12 and the upper curve of Fig. 14 both show more gradual increase in phase contamination as weir pressure approaches the theoretical curve than is typical at O/A values of unity. This is seen in the increasing number of experimental points in the range of 1-2% phase contamination, which, in these two cases, represents contamination in the continuous phase.

This picture of a dispersion band without a distinct boundary agrees with earlier findings [BARNEA] for a continuous-flow gravity settler in that the range for a distinct dispersion band is between O/A values of 0.28 and 3.5.

~~OFFICIAL USE ONLY~~

At the same time, this present work shows that the dispersion-band model and contactor operation are not limited to that range of O/A values where a distinct interface exists between the dispersion band and the separated phases.

D. Liquid Height in the Couette Mixing Zone

Experimental data on the liquid height in the Couette (annular) mixing zone were obtained using a perpendicular tap in the contactor housing with its centerline at 28 mm above the bottom of the rotor. The inside diameter of the tap is 9.2 mm. At higher liquid levels, a second tap with its centerline at 105 mm above the bottom of the rotor was also used. The results in Fig. 16 show how liquid height in the Couette mixing zone varies with rotor speed at various throughputs.

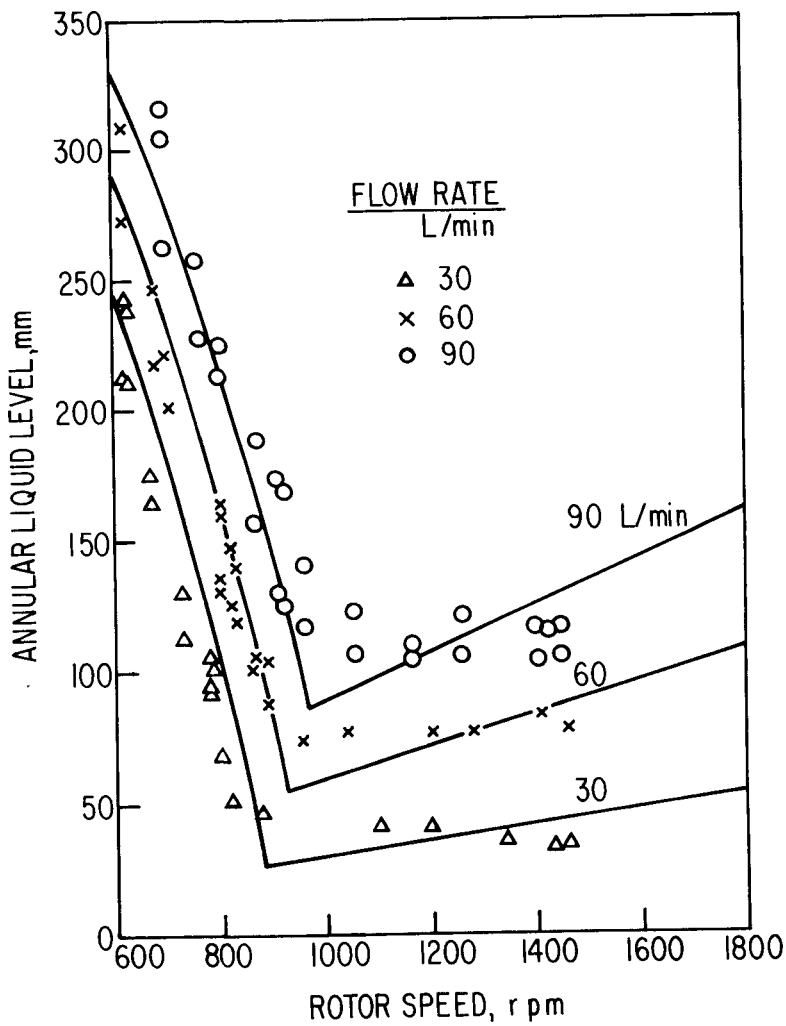

Fig. 16. Effect of Flow Rate and Rotor Speed on the Liquid Level in the Couette (Annular) Mixing Zone. [25-cm Contactor; A: 0.3 M HNO_3, O: 30% TBP in nDD, O/A = 1.0. Solid curves are based on semi-theoretical correlation.]

OFFICIAL USE ONLY

In essence, the liquid height decreases as rotor speed decreases until the rotor is not fully pumping. Below this rotor speed, the liquid height rises sharply.

For these tests, a semi-theoretical correlation has been developed which is shown as the solid curves in Fig. 16. The basis for the correlation is that the total annular liquid height above the bottom of the rotor, H, is the sum of the expected height, H_1, if the rotor is fully pumping, plus the liquid head, H_2, required to make up the difference between what the rotor can pump and the length, b_o, of the separating zone of the rotor. Earlier work with the 9-cm contactor showed that H_1 is proportional to the flow rate, q, and the rotor speed, ω. For the 1200- to 1450-rpm data given here, this gives

$$H_1 = k_1 \, q \, \omega \tag{4}$$

where k_1 is a constant equal to 0.57 s^2/m^2. H_2 is the difference between the length of the separating zone and the hydraulic pumping head of the rotor and is given by

$$H_2 = \begin{cases} b_o - \frac{\omega^2}{2g}(r_o^2 - r_t^2) \\ \\ 0 \text{ if } b_o \leq \frac{\omega^2}{2g}(r_o^2 - r_t^2) \end{cases} \tag{5}$$

where r_t is the radius of the rotor inlet on the bottom face of the rotor and r_o is the radius of the liquid surface over the organic weir. Notice that the liquid rise over the organic weir is also needed in this calculation. The inertial head required to force the liquid into the rotor can be neglected. In general, Fig. 16 shows good agreement between the semi-theoretical correlation and the experimental data.

Some slight deviation can be seen between the correlation and the data in Fig. 16 at the transition between a partially- and a fully-pumping rotor. The semi-theoretical correlation predicts a sharp break while the data show a more gradual change. This deviation is not due to the improper use of r_t since a decrease in r_t of 0.5 mm at 1000-rpm rotor speed would change H_2 by 20 mm, that is, by the amount of the deviation in the transition region. A possible explanation is that it is difficult for entrained air which disengages from the dispersion under the diverter disk in the rotor to go through the vent holes in the disk. This happens because the liquid at the bottom of the rotor at the transition region is at the radius of the rotor inlet (38.1 mm) while the 6.4-mm-dia vent holes lie between inner and outer radii of 37.3 mm and

~~OFFICIAL USE ONLY~~

43.7 mm, respectively. Additional pressure to force the air through these vent holes would be reflected in a higher liquid level in the Couette mixing zone. The data suggest this pressure to be on the order of 14 to 20 mm of liquid at the transition point. If this explanation is valid, placing vent holes closer to the rotor axis should eliminate the small difference between the correlation and the experimental data. However, as a practical consideration, the added pressure needed to force the air through the vent holes does not affect the overall performance of the contactor.

In one further test series, the effect of the vane-to-rotor gap was tested by increasing the gap from its normal 0.8-mm value to 8.8 mm. Tests in the fully pumping region, 1200 to 1450 rpm, show that the liquid height in the annulus was unchanged at 30 L/min, increased 28% at 60 L/min, and increased 44% at 90 L/min. In no case was the liquid level in the Couette mixing zone close to the organic collector ring whose lip is 412 mm above the bottom of the rotor. Thus, the operation of this contactor in a multi-stage array would not be obstructed by high liquid levels in the interstage lines even if the vane-to-rotor gap was abnormally high.

E. Contactor Capacity

Since the liquid level in the Couette mixing zone is low, contactor capacity is determined by the dispersion number, N_{Di}, of the dispersion coming from the Couette mixing zone into the separating zone of the rotor. Further, as shown in Table 4, N_{Di} is unaffected by rotor speed so that contactor capacity should be proportional to the rotor speed. This relationship was tested, as shown in Fig. 17, and found to be valid.

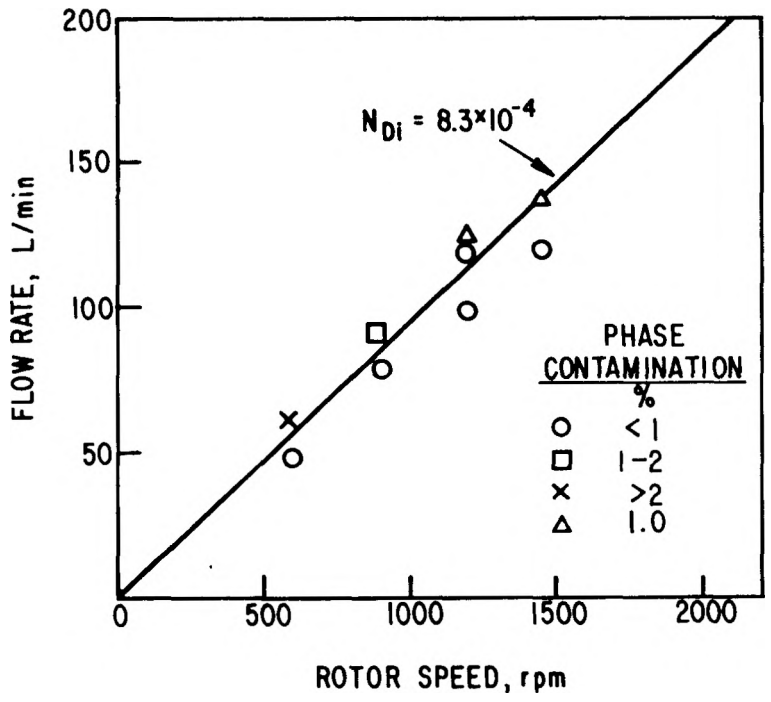

Fig. 17. Effect of Rotor Speed on 25-cm Contactor Capacity. (A: 0.3M HNO_3, O: 30% TBP in nDD, O/A = 1.0. Note: Results for 1.0% phase contamination were extrapolated from data at lower flow rates.)

OFFICIAL USE ONLY

Using the slope of this curve along with the average separating-zone radius, $\bar{r}$, of 0.0915 m, the thickness of the separating zone, ΔZ, of 0.0716 m, and the volume of the separating zone, V, of 0.01614 m^3, the dispersion number can be calculated using

$$N_{Di} = \frac{q}{V} \sqrt{\frac{\Delta Z}{\bar{r}\omega^2}} \tag{6}$$

to obtain 8.3×10^{-4}. This N_{Di} value agrees with N_{Di} measurements given in Section B above.

From the dispersion-band model, the aqueous weir pressure required for maximum throughput can also be calculated as a function of rotor speed and throughput for various O/A ratios. Model results for an O/A ratio of 1.0 are shown in Fig. 18 as the solid curves along with four experimental points.

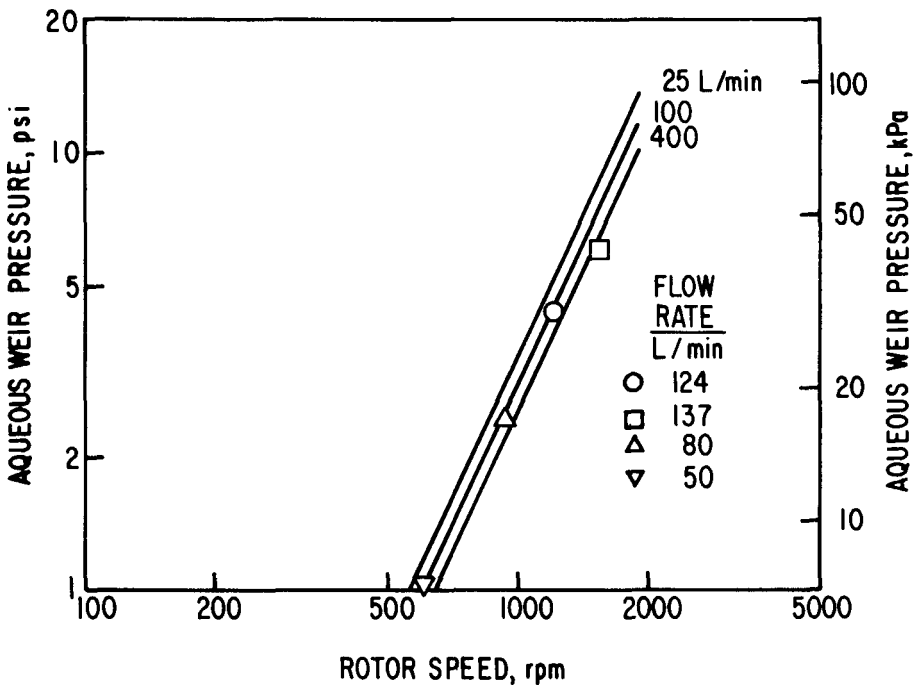

Fig. 18. Effect of Rotor Speed on Aqueous Weir Pressure for Various 25-cm Contactor Capacities. (A: 0.3M HNO_3, O: 30% TBP in nDD, O/A = 1.0. Note: Solid curves show dispersion-band model results with equal volumes of each phase in the dispersion band.)

~~OFFICIAL USE ONLY~~

Again, agreement between theory and experiment is good. At higher O/A ratios, the dispersion band is less dense so that higher aqueous weir pressures are required; at lower O/A ratios, the dispersion band is more dense so that lower pressures are required.

V. MIXING POWER

Major power requirements for the annular centrifugal contactor, above that required to operate the rotor and motorized spindle without any liquid, are (1) the power dissipated in the Couette (annular) mixing zone, (2) the power to accelerate the liquids in the separating zone, (3) the power to lift the liquid the length of the separating zone, and (4) the power dissipated under the rotor. A method for calculating the mixing power, P_1, in the Couette zone has been developed [LEONARD-D] as

$$P_1 = 0.0261 \left[\frac{H\, r_{R,o}^{3.75}\, (j\omega)^{2.75}\, \rho^{0.75}\, \mu^{0.25}}{\Delta r_c^{0.25}} \right] \tag{7}$$

where H = liquid height in Couette mixing zone, m

$j = 0.0554 \log N_{Re} + 1.368$

$N_{Re} = 3.2\, \omega \rho r_{R,o}\, \Delta r_c / \mu$

P_1 = Couette-zone mixing power requirements, W

$\Delta r_c = r_{H,i} - r_{R,o}$, m

$r_{H,i}$ = inside radius of the housing, m

$r_{R,o}$ = outside radius of the rotor, m

μ = dispersion viscosity, Pa·s

ρ = dispersion density, kg/m^3

ω = rotor rotational velocity, rad/s

The power, P_2, in W, to accelerate the dispersion in the rotor is given by

$$P_2 = \frac{1}{2} \rho r_{R,o}^2\, \omega^2 q \tag{8}$$

where q = flow rate, m^3/s. The power, P_3 in W, to lift the liquids the height

OFFICIAL USE ONLY

of the separating zone is given by

$$P_3 = \rho g b_o q \tag{9}$$

where

b_o = height of separating zone, m

g = gravitational acceleration, m/s^2

The power dissipated under the rotor was neglected in the calculations.

Power requirements for various rotor speeds and throughputs were measured and are listed in Table 5 along with the power for no liquid in the contactor and the calculated power to accelerate and lift the liquids. From this, a mixing power is calculated and plotted in Fig. 19 as a function of $\omega^{2.75}H$ which is the only part of the Couette mixing power which varies for a given

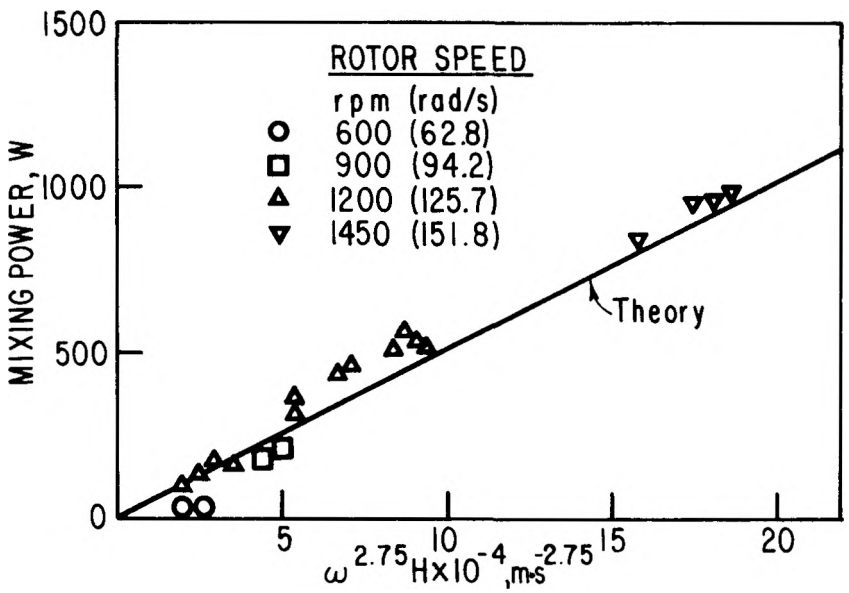

Fig. 19. Correlation of Mixing Power with the Operating Parameters of the 25-cm Contactor. (A: 0.3M HNO_3, O: 30% TBP in nDD, O/A = 1.0.)

contactor. The theoretical curve given by Eq. 7 is plotted in Fig. 19 along with the experimental data and reasonable agreement is seen. For the theoretical curve, the dispersion viscosity is assumed to be that of the continuous phase.

~~OFFICIAL USE ONLY~~

Table 5. Contactor Power Requirements

Test conditions: 25-cm Contactor
A: 0.3M HNO_3
O: 30% TBP in nDD
O/A = 1.0

Power for motor plus
empty rotor is 200 W
at 1200 rpm (125.7 rad/s)

Rotor Speed, rpm (rad/s)	Flow Rate, L/min	Liquid Height in Couette Mixing Zone, m	Measured Total Power, W	Calculated Pumping Power, W	Calculated Power to Accelerate Fluid in Rotor, W
600 (62.8)	50	0.284	240	3	29
600 (62.8)	60	0.284	250	4	35
900 (94.2)	80	0.162	500	5	106
900 (94.2)	90	.161	515	6	119
1200 (125.7)	40	0.042	430	2	94
1200 (125.7)	40	.034	400	2	94
1200 (125.7)	40	.060	460	2	94
1200 (125.7)	40	.042	450	2	94
1200 (125.7)	80	.092	710	5	188
1200 (125.7)	80	.091	760	5	188
1200 (125.7)	100	.112	870	6	235
1200 (125.7)	100	.118	900	6	235
1200 (125.7)	113	.142	960	7	266
1200 (125.7)	120	.149	1050	7	282
1200 (125.7)	120	.153	1020	7	282
1200 (125.7)	120	.158	1000	7	282
1450 (151.8)	127	0.182	1600	8	436
1450 (151.8)	125	0.182	1600	8	429
1450 (151.8)	125	.177	1600	8	429
1450 (151.8)	120	.159	1450	8	411

Some errors are expected in the data shown in Fig. 19 because the industrial analyzer (Model TA, Westinghouse Electric Corp, Pittsburgh PA) used to measure power was operating at the low end of its scale which is marked in 200-W increments and can be read to only ±50 W. A further source of error is that the power required to run the rotor empty was measured only one time at one rotor speed, 1200 rpm. This is probably the reason why the 600-rpm power

~~OFFICIAL USE ONLY~~

readings are so far below the theoretical line. An estimate of the power dissipated under the rotor indicates it should be equivalent to the Couette mixing power when the height of liquid in the Couette zone increases by an amount which is 20% of the radius of the rotor. Thus at 1200 rpm, where annular-zone liquid height is close to its minimum, the effect of power dissipated under the rotor should be most significant and could increase the actual mixing power by as much as 20% above the theoretical curve. This is, in fact, seen to be roughly the case at 1200 rpm where the experimental data lie as much as 20% above the theoretical curve. At the higher rotor speed, 1450 rpm, where the height in the Couette zone is greater, the data are closer to the theoretical curve. Since the height of liquid also rises at lower speeds, data at 600 and 900 rpm should also be closer to the theoretical curve. However, because of experimental errors in the power measurements, agreement below 200 W of mixing power is not very reliable and this hypothesis cannot be properly tested.

VI. DISCUSSION

Since contactor capacity exceeded the pumping capacity of the available feed system, contactor capacity could only be demonstrated up to 120 L/min. However, the dispersion number correlation as given in Fig. 17 indicates a current contactor capacity of 137 L/min at a rotor speed of 1450 rpm. If the maximum allowable rotor speed can be increased substantially so that operation at 1800 rpm would no longer cause high vibrational velocities over 2.5 mm/s (0.1 in./s), then, as indicated in Fig. 17, contactor capacity would be 170 L/min (2.83×10^{-3} m^3/s). At 1800 rpm, Eq. 4 gives a height in the Couette (annular) mixing zone of 0.304 m which means that 74% of the mixing zone is filled. Extrapolation of the curve in Fig. 19 gives the required mixing power as 2.70 kW with additional power required to accelerate the liquid (0.81 kW), lift the liquid (0.01 kW), and run the system empty (0.20 kW); thus, the total power required at 1800 rpm would be 3.72 kW which is essentially the capacity of the 3.73-kW (5-hp) motorized spindle. The use of a 5.6-kW (7.5-hp) motorized spindle would provide some reserve power for operating at a nominal rotor speed of 1800 rpm. Operation at a nominal 1800 rpm is desirable since this would increase contactor capacity and eliminate the need for a variable-frequency generator.

ACKNOWLEDGMENTS

The authors wish to acknowledge the help of E. M. Rudnick and R. H. Pelto in making the 25-cm contactor tests and of M. A. Slawecki in setting up the variable-frequency generator and the power meter. The authors also wish to acknowledge the support and interest of M. S. Steindler, D. S. Webster, and L. Burris.

~~OFFICIAL USE ONLY~~

REFERENCES

BARNEA

E. Barnea and J. Mizrahi, Separation Mechanism of Liquid-Liquid Dispersions in a Deep-Layer Gravity Settler, Trans. Inst. Chem. Eng. 53, 61-92 (1975).

BERNSTEIN

G. J. Bernstein, D. E. Grosvenor, J. F. Lenc, and N. M. Levitz, A High-Capacity Annular Centrifugal Contactor, Nucl. Technol. 20, 200-202 (1973).

BRAND

L. Brand, Vectorial Mechanics, Wiley, NY (1930).

KISHBAUGH

A. A. Kishbaugh, Performance of a Multistage Centrifugal Contactor, DP-841 (October 1963).

LEONARD-A

R. A. Leonard, G. J. Bernstein, A. A. Ziegler, and R. H. Pelto, Annular Centrifugal Contactors for Solvent Extraction, Sep. Sci. Technol. (accepted for publication).

LEONARD-B

R. A. Leonard, R. H. Pelto, A. A. Ziegler, and G. J. Bernstein, Flow over Circular Weirs in a Centrifugal Field, Can. J. Chem. Eng. (accepted for publication).

LEONARD-C

R. A. Leonard, G. J. Bernstein, R. H. Pelto, and A. A. Ziegler, Liquid-Liquid Dispersion in Turbulent Couette Flow, presented at the 72nd Annual Meeting of the AIChE, San Francisco, CA, Nov. 25-29, 1979 (submitted to the AIChE Journal for publication).

LEONARD-D

R. A. Leonard, Prediction of Hydraulic Performance in Annular Centrifugal Contactors, Argonne National Laboratory Report (in preparation).

RANEY

M. S. Raney, Ed., Spent LWR Fuel Recycle Complex, DP-CFP-79-121 (September 1979).

WEBSTER

D. S. Webster, A. S. Jennings, A. A. Kishbaugh, and H. K. Bethmann, Performance of Centrifugal Mixer-Settler in the Reprocessing of Nuclear Fuel, AIChE Chem. Eng. Prog. Symp. Ser., Nuclear Engineering--Part XX, No. 94, Vol. 65, pp 70-77 (1969).

~~OFFICIAL USE ONLY~~

Distribution for ANL-80-15

Internal:

W. E. Massey
E. S. Beckjord
C. E. Till
R. Avery
L. Burris
D. W. Cissel
S. A. Davis
B. R. T. Frost
E. V. Krivanec
L. G. LeSage
D. E. Simpson
R. J. Teunis
R. S. Zeno
R. A. Leonard (15)
G. J. Bernstein
J. E. Harmon
A. Melton
R. H. Pelto
P. Raptis
J. W. Simmons
M. J. Steindler (3)
D. S. Webster
A. A. Ziegler
ANL Contract File
ANL Libraries (2)
TIS Files (6)

External:

DOE-TIC, for distribution per UC-86 (105)
Manager, Chicago Operations and Regional Office, DOE
Chief, Office of Patent Counsel, DOE-CORO
Director, Technology Management, DOE-CORO
President, Argonne Universities Association
Chemical Engineering Division Review Committee:
C. B. Alcock, U. Toronto
R. C. Axtmann, Princeton U.
J. T. Banchero, U. Notre Dame
T. Cole, Jet Propulsion Lab.
P. W. Gilles, U. Kansas
R. I. Newman, Warren, N. J.
H. Perry, Resources for the Future, Washington
G. M. Rosenblatt, Pennsylvania State U.

~~OFFICIAL USE ONLY~~